Progress In Electromagnetics Research, Vol. 136, 647–664, 2013

MAGNETIC FIELD SHIELDING BY METAMATERIALS

Mustafa Boyvat* **and Christian Hafner**

Department of Information Technology and Electrical Engineering, ETH Zurich, Gloriastrasse 35, Zurich 8092, Switzerland

Abstract—Magnetic field shielding at low frequencies is a problem of high importance that is known for a long time. Metamaterials, which are known from fancy applications such as the so-called perfect lens and cloaking, also offer a new way to create efficient magnetic shielding by means of anisotropic metamaterials with low permeability in one direction. Such metamaterials can be constructed by assembling arrays of relatively simple LC circuits. In this paper, we analyze different metamaterials and show how they may be designed. We show that typical resistive losses in the coils and capacitors of the LC circuits reduce the shielding quality. Then, we consider the possibility of active electronic loss compensation and discuss the drawbacks of this concept. After this, we propose a purely passive way that benefits from the inhomogeneity of the magnetic field to be shielded. Finally, we present experimental results, which show the performance of metamaterial shields.

1. INTRODUCTION

Metamaterials are materials which can provide unusual or extraordinarily strong electromagnetic properties, which cannot be found in natural materials [1, 2]. In 2000, Pendry theoretically showed that one can make a perfect lens, which is not limited by diffraction limit, by using metamaterials with negative permittivity and negative permeability [3]. After this, metamaterials attracted much attention and also experimental work has been done to demonstrate negative refraction and superlensing effects [4–9]. Another milestone in metamaterial history has been the cloaking of an object, i.e., making an object invisible by surrounding it with a metamaterial shield [10]. Note that such

Received 18 December 2012, Accepted 21 January 2013, Scheduled 30 January 2013

* Corresponding author: Mustafa Boyvat (mustafa.boyvat@ifh.ee.ethz.ch).

a shield needs to be inhomogeneous, while the super lens is a simple, homogeneous metamaterial slab. In principle, one guides light around the object by transformation optics [10].

It should be mentioned that most of the work on metamaterials has focused on high frequencies such as microwaves up to optical waves. The main reason for this is that some features of the metamaterial must couple the electromagnetic fields inside the metamaterial with the fields outside. Otherwise, a metamaterial block would not interact with the surrounding material. This is usually done by some sort of antennas that become huge at low frequencies. For example, in negative index metamaterials, so-called split ring resonators are often used [2]. They do not only provide the desired properties of the metamaterial but they also act as loop antennas that couple the field inside the metamaterial with the field outside. Incidentally, it is well known from antenna theory that efficient antennas cannot be much smaller than the wavelength of the surrounding domain. As a result, the antenna size increases with the wavelength.

At sufficiently low frequencies, the coupling between electric and magnetic fields becomes weak. Then simple coils provide the desired coupling of the magnetic (but not electric) fields inside the metamaterial with the magnetic fields outside, i.e., manipulating magnetic fields inside a metamaterial containing coils that are much smaller than the wavelength is possible at low frequencies due to magnetic induction.

Magnetic field produced by power transformer stations and power cables in residential areas has to be shielded because of regulations [11] that depend very much on the country. Since these regulations became stricter in some countries, e.g., Italy and Switzerland, there is a need for finding improved magnetic field shields. Recently, it has been shown that metamaterials can indeed be used to shield magnetic fields at very low frequencies [12].

Similar to natural materials, which are composed of atoms and molecules, metamaterials are composed of subwavelength units, which are called 'meta-atoms' [1]. In order to provide strong effects, meta-atoms must be resonating structures, which typically come with high loss and narrow bandwidth, being two major issues of metamaterials [13, 14]. There have been attempts to overcome these problems by using active elements. When the frequency is low enough, large wavelengths allow one to use lumped elements such as inductors and capacitors but also electronic parts in a meta-atom [15–21]. In this paper, we first discuss the basic principles of a magnetic meta-atom and the concepts to improve its response. Then we explain the drawbacks of active circuits for loss compensation and we propose a

new, purely passive method that is benefiting from the inhomogeneity of the source magnetic field.

2. SHIELDING PRINCIPLE OF A MAGNETIC META-ATOM

When the frequency is very low, a meta-atom, which must have subwavelength size, can be manufactured rather easily because of the long wavelength. For example, it can consist of a simple LC resonator consisting of standard lumped circuit elements, i.e., a coil and a capacitor as shown in Figure 1, whereas its optical analogue requires advanced fabrication techniques [22, 23].

For the analysis, the quasi-static approximation can be used and this simplifies the metamaterial analysis considerably. The working principle of an LC resonator as a meta-atom can be explained as follows:

The coupling to the field happens through the inductor, i.e., the coil. When there is a time varying magnetic field through a conductive loop, a current is induced on the loop and this current is given by

$$I = -j\omega\phi/(Z_{load} + Z_{loop}) \tag{1}$$

where ω is the angular frequency, ϕ the magnetic flux through the coil, caused by the source and the other meta-atoms, and Z_{load} and Z_{loop} are the impedances of the load connected to the coil and the coil itself respectively [24]. This current also produces a magnetic field and total magnetic field at a point in space is the superposition of the source magnetic field and the fields caused by all meta-atoms. When the meta-atom is a simple LC resonator with some resistance, the total impedance and the current in the resonator are given by the following

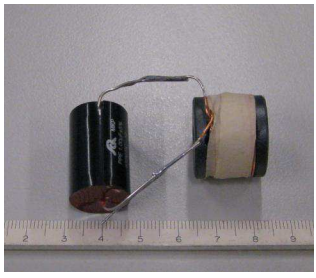

Figure 1. A meta-atom at low frequencies, composed of a capacitor (1 µF) and a coil (1 mH).

relations [24]:

$$Z_{total} = Z_{load} + Z_{loop} = j\omega L + 1/(j\omega C) + R \tag{2}$$

$$I_{res} = \frac{-j\omega \int \overrightarrow{B_{ext}} \cdot d\vec{S}}{j\omega L + 1/(j\omega C) + R} \tag{3}$$

When the meta-atom size is small enough, $\overrightarrow{B_{ext}}$ can be assumed to be uniform in a meta-atom and the relation between the resonator current and the external magnetic field can be written as $I_{res} = \alpha \cdot B_{ext,n}$. Here, $B_{ext,n}$ is the axial component of the external magnetic flux density at the center of the coil and α is $j\omega A/(j\omega L + 1/(j\omega C) + R)$, where A is the area of the loop. When R is 0, the resonator produces in-phase magnetic field with the external magnetic field just below the resonance frequency, thus enhances the magnetic field, whereas it is in opposite phase just above resonance frequency and reduces the magnetic field if its magnitude is less than the double of the external magnetic flux density. When there is a non-zero resistance, one can still observe enhancement below resonance frequency and shielding above resonance frequency, but the magnetic field produced by the meta-atom can never have exactly 0 or 180 degree phase difference with respect to the incident field. The field enhancement and reduction mechanism of a meta-atom can be seen in the phasor diagram shown in Figure 2.

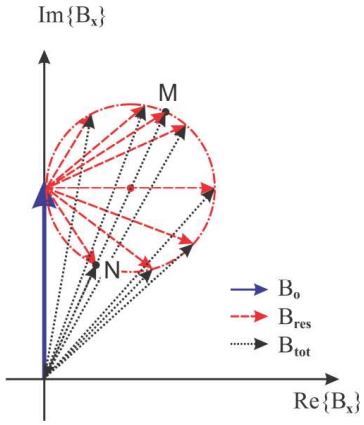

Figure 2. Response of an RLC meta-atom: Phasors of the source (blue, continuous), resonator (red, dashed), and total (black, dotted) magnetic flux density. The circle is the trace of meta-atom magnetic flux density for frequencies from 0 to infinity [12]. M and N points show the points at which the total magnetic flux density is maximum and minimum respectively.

B_x is the x component of magnetic flux density, at a point in space where x axis is the axes through the coil. B_0 represents the external magnetic flux density, B_{res} is the field produced by the meta-atom, and B_{tot} is the total magnetic flux density. When the frequency changes, the magnitude and the phase of the current in the coil, thus the magnitude and the phase of the magnetic flux density produced by the meta-atom changes. The circle shown in Figure 2 is the trace of the resonator magnetic flux density phasor when the frequency is swept from 0 to infinity. At DC, the resonator magnetic flux density is zero and the resonator flux density phasor sits at the tip of B_0. When frequency increases, the tip of the resonator flux density follows the red circle in clock-wise direction. At resonance, the magnitude of the current in the resonator and the resonator magnetic flux density reaches its maximum value. At this frequency, the magnetic flux density produced by the meta-atom has 90 degree phase difference with the external magnetic flux density and the superposition of these two gives more magnitude than the external flux density, which means there is a field enhancement. However, having maximum resonator current does not mean the maximum total flux density because of the phase difference. Maximum enhancement occurs at a frequency below resonance frequency, where B_{tot} reaches its maximum, which is shown by point M in Figure 2. Similarly, maximum reduction occurs at a frequency above resonance frequency, where B_{tot} reaches its minimum, as shown by point N in Figure 2. When another point in space is taken, because the weights of external and meta-atom flux densities change, these two frequencies at which the maximum enhancement and reduction happen also change, although they are still below and above the resonance frequency respectively.

The maximum and minimum flux densities can be found using geometrical properties. If we call the maximum resonator magnetic flux density $B_{x,res,\max}$, which is the diameter of the circle in the phasor diagram, the maximum and minimum flux densities are given by the following relations:

The maximum x component of total magnetic flux density (see M point in Figure 2) is given by

$$B_{x,\max} = \sqrt{B_0^2 + B_{x,res,\max}^2/4} + B_{x,res,\max}/2 \tag{4}$$

and the minimum x component of total magnetic flux density (see N point in Figure 2) is given by

$$B_{x,\min} = \sqrt{B_0^2 + B_{x,res,\max}^2/4} - B_{x,res,\max}/2 \tag{5}$$

It can be seen that the maximum enhancement percentage is always larger than the maximum reduction percentage. Also it is obvious that

it is never possible to have zero magnetic flux density with a non-zero resistance.

3. IMPROVED META-ATOM WITH ACTIVE CIRCUITS

For non-zero resistance R, a single RLC can never shield the magnetic field perfectly, i.e., make it zero near the coil. An obvious improvement is obtained when L and C components with very low resistive values are used. Then, the magnetic flux density circle of the resonator in the phasor diagram enlarges and improves shielding (see Figure 2). However, this idea is not feasible in practice because decreasing the resistance of coils considerably requires much thicker wires, i.e., heavy, large, and expensive coils. Obviously, superconducting coils would also provide high costs and additional problems. Furthermore, the reduction of R also reduces the bandwidth of the RLC circuits, which makes its tuning much more difficult.

A common method to improve the meta-atoms is to use active circuits [15, 19–21], for example, by using negative impedance converters. However, active circuits may have serious problems such as stability [19, 25] and the requirement of an external power source. Moreover, they need cooling when they need to provide large currents if the source field is not very weak. As a result, one obtains bulky and expensive meta-atoms. A realization of an active circuit to improve the meta-atom in kHz range can be seen in [26] and Figure 3.

4. IMPROVED META-ATOM WITH ADVANCED PASSIVE CIRCUITRY

In principle, the magnetic field of the source to be shielded already provides energy that may be delivered to the meta-atom. Thus, an external power source — as mentioned in the previous section — is not really needed. One can simply use an additional coil that delivers the energy needed by the electronic circuit. In this case, the problem of huge currents in the active circuit remains.

A more promising alternative is to take advantage of a second coil in a purely passive circuit. Namely, one can use a second coil connected in series and locate it closer to the source than the first one. As a consequence, more magnetic flux couples into the meta-atom, and more current is induced. To keep the resonance frequency constant, also a second capacitor is added in series. This makes it possible to enhance the response of the meta-atom whereas the change in the bandwidth may be kept small compared to the gain in the meta-atom response.

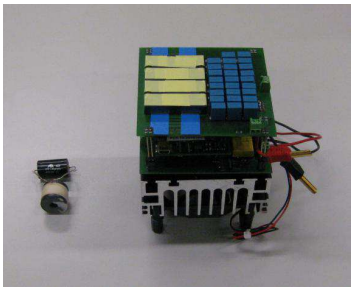

Figure 3. Comparison of the sizes of an active circuit to improve the meta-atom and an RLC meta-atom.

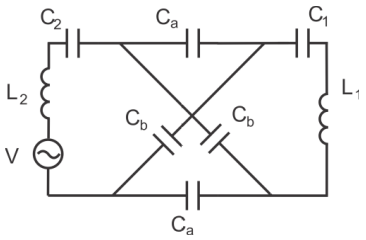

Figure 4. The advanced passive circuit.

The meta-atom then resembles an ideal LC meta-atom more, but still it is not possible to design a circuit with two capacitors and two inductors in such a way that the magnetic flux has a phase exactly opposite to the magnetic flux of the source. In order to realize perfectly opposite phase, the magnetic flux density circle in the phasor diagram (Figure 2) needs to be rotated by -90 degrees. This rotation also eliminates the huge field enhancement due to the enhanced current in the meta-atom below resonance frequency.

To introduce a phase shift in a signal, a 'Lattice Phase Equalizer', which is composed of inductors and capacitors is used [27, 28]. By combining the idea of using the lattice phase equalizer and using a second coil, the advanced passive circuit in Figure 4 is obtained. As one may see, there are two inductors, one of which is close to the source, and four capacitors. More inductors have been avoided because the interaction of those inductors with the magnetic field must be considered and this makes the design more complicated and difficult.

There are two assumptions to simplify the analysis of shielding by the advanced passive circuit. The first one is that the induced voltage is only in the inductor which is close to the source, thus the induced voltage in the other coil is neglected. The second assumption is that the inductor which is close to the source does not contribute to the meta-atom magnetic field in the region to be shielded because it is far away from the region to be shielded.

To obtain the necessary phase shift, the following relation needs to be satisfied at the frequency at which the phase is $-90°$:

$$I_{ind,1} = -jV/(k.R) \tag{6}$$

where V is the induced voltage in the circuit, $I_{ind,1}$ is the current in the inductor which is further from the source, R is the resistance in the initial RLC circuit and k is a positive real number.

Usually, the operation frequency of the metamaterial is given and the R, L, C values must be optimized. For demonstrating the metamaterial performance, we can set the resonance frequency to any value, i.e., we can take any commercially available inductance and capacitance values and measure or compute the resulting resonance frequency. The circuit was designed to have the relation in Equation (6) with reasonable component values considering also the approximate series resistances of components at the frequency for which it is designed. The resistance values are the measured values around the operation frequency of the metamaterial. In the end, the component values were rounded to commercially available values. C_1, C_2, C_a, C_b, R_1, R_2, R_a, R_b values in the final design are given below. R_1 is the resistance of the coil which is close to the source, R_2 is the resistance of the further coil from the source, R_a is the equivalent series resistance of C_a, R_b is the equivalent series resistance of C_b. The equivalent series resistances of C_1 and C_2 are negligible because of the high quality of those capacitors.

$$C_1 = 1\,\mu F, \quad C_2 = 1\,\mu F, \quad C_a = 100\,\mu F, \quad C_b = 10\,\mu F,$$
$$R_1 = 1.31\,\Omega, \quad R_2 = 1.31\,\Omega, \quad R_a = 0.2\,\Omega, \quad R_b = 0.37\,\Omega$$

An RLC and the advanced passive circuit were simulated for comparison and verification. Both were fed by 1 V with 0 phase and the frequency characteristics of both circuits were obtained sweeping the frequency. The phasor representations of currents of both circuits can be seen in Figure 5. In the advanced passive circuit, the current through the coil further away from the source, or in other words, closer to the region to be shielded, is plotted. From the simulation, we see that the k value of the finalized design is 2.45 (See Equation (6)).

5. EXPERIMENTAL DEMONSTRATION OF SHIELDING BY METAMATERIALS

5.1. Metamaterial Composed of Simple RLC Meta-atoms

To measure the performance of simple RLC meta-atoms, an array of 16 meta-atoms is used. The meta-atoms were LC resonators formed by coils with inductance 1 mH and capacitors with 1 μF capacitance. The array is mounted on a square lattice with a distance of 4 cm between neighbor elements. The source is a rectangular coil with the size of 27 cm by 20.1 cm. The array is placed at 14 cm from the source. An illustration of the experimental setup can be seen in Figure 6.

The frequency characteristic of the metamaterial is shown in Figure 7. A Narda EFA-300 Field Analyzer with a 3 cm probe was used to measure the magnetic flux density. The magnetic field probe

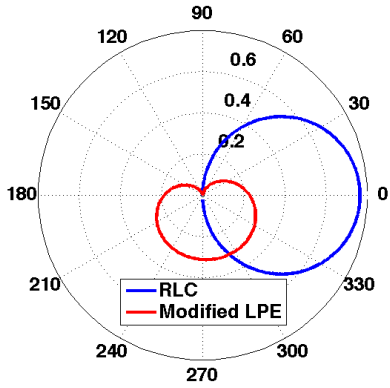

Figure 5. The trace of the current phasors with changing frequency for an RLC circuit and the advanced passive circuit. It is known that the magnetic flux density produced by meta-atom is proportional to the current on the meta-atom and that the magnetic flux density produced by the meta-atom and the current are in phase, thus this diagram is a direct indication of the meta-atom magnetic flux density. The voltage sources in both circuits have 1 V magnitude and 0 phase. The lattice phase equalizer circuit rotates the circle in the diagram corresponding to the RLC circuit with some shape change which is not important and makes opposite phase to the source magnetic flux density possible (See Figure 2).

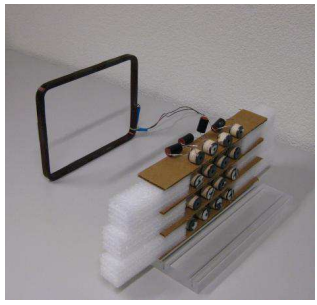

Figure 6. An illustration of the experimental setup for a metamaterial built by RLC meta-atoms. The large coil is used as magnetic field source and the metamaterial is a 4×4 array of coil and capacitor pairs.

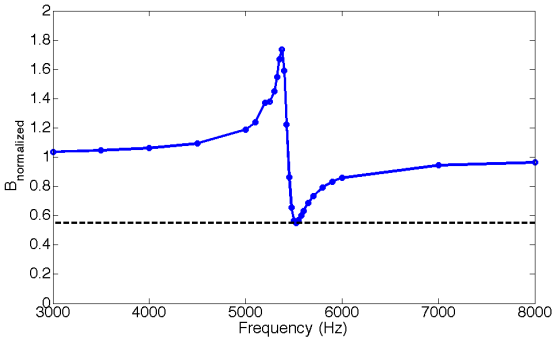

Figure 7. Frequency response of a metamaterial built by RLC resonators. $B_{\text{normalized}}$ is the magnetic flux density normalized to the source magnetic flux density. First, it is seen that metamaterial shows an enhancement reaching up to 73%, and when the frequency increases it starts to shield and maximum shielding is 45% at the point where the frequency response was measured.

was placed at 30.5 cm from the source and the frequency dependence of the normalized magnetic flux density was obtained. To verify that the observed effects are not due to the change in the current through the source coil due to back-coupling, the current through the source coil was measured with and without the metamaterial shield and a negligible difference in current values was seen.

In the field-frequency curve, we first see a field enhancement up to 73%. When the frequency increases the metamaterial starts to shield and maximum shielding of 45% is obtained. The bandwidth in which the shielding stays more than 70% of its maximum is 171 Hz. However the frequency characteristic around the optimum shielding frequency is not symmetric and the shielding drops to 70% of its maximum within 54 Hz towards lower frequencies. The resonance frequency of a single resonator is calculated to be 5034 Hz. The frequency response curve is shifted to higher frequencies due to negative mutual coupling between elements [29]. To have an intuition about this shift, one can imagine two identical meta-atoms placed symmetrically so that they have the same flux through them and carry the same current.

$$I_{res,1} \cdot (j\omega L + 1/(j\omega C) + R) + I_{res,2} \cdot j\omega M = -j\omega\phi_1 \tag{7}$$

$$I_{res,2} \cdot (j\omega L + 1/(j\omega C) + R) + I_{res,1} \cdot j\omega M = -j\omega\phi_2 \tag{8}$$

Because of the assumed symmetry, $\phi_1 = \phi_2$ and $I_{res,1} = I_{res,2}$. Thus two equations become identical and take the following form:

$$I_{res} \cdot (j\omega(L + M) + 1/(j\omega C) + R) = -j\omega\phi \tag{9}$$

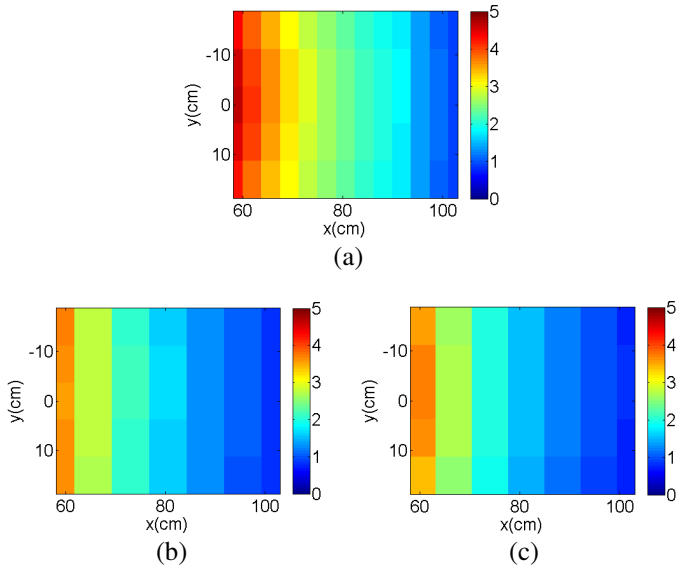

Figure 8. The spatial distribution of magnetic flux density without and with metamaterial. The color shows the magnetic flux density in μT. The source coil is at $(x = 0, y = 0)$. (a) The magnetic flux density of the source coil. (b) The magnetic flux density with the metamaterial located at $x = 14$ cm. (c) The magnetic flux density with the metamaterial located at $x = 38$ cm.

Negative mutual coupling effectively decreases the inductance term in the equation, thus increases the resonance frequency.

The spatial distribution of the magnetic flux density in the horizontal plane at the level of the center of the metamaterial layer was also measured. The shielding performance of the metamaterial layer can be seen in Figure 8.

5.2. Metamaterial Composed of Two Coil Layers and Phase Lattice Equalizer

A metamaterial was built to demonstrate the improvement by two coil layers and the phase lattice equalizer circuits experimentally. (The new meta-atom can be seen in Figure 9). The first coil layer was placed at 38 cm from the source coil and the secondary coil layer, which is close to the source, were placed at 14 cm from the source. With two additional coils, one to measure the phase of the source magnetic flux

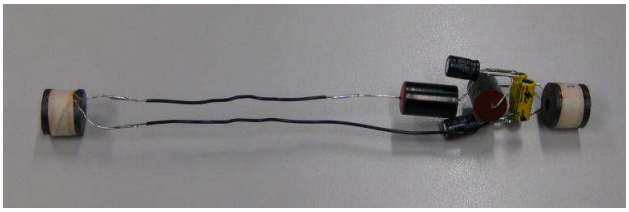

Figure 9. Meta-atom with two coils and the lattice phase equalizer circuit.

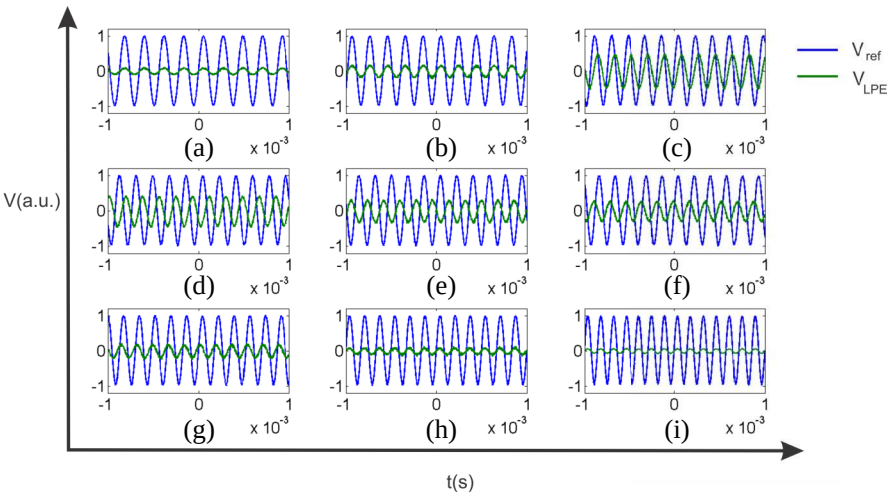

Figure 10. The phase of magnetic flux density at different frequencies from (a) 5100 Hz to (i) 7000 Hz. The magnetic flux density is observed in time domain by using coils and monitoring the induced voltages on them. V_{ref} is the normalized voltage on the coil placed very close to the source coil and V_{LPE} is the normalized voltage on the coil placed in the region to be shielded. It is seen that the phase of the magnetic flux density is first almost in-phase with the source magnetic flux density and with increasing frequency it passes through 180°.

density and the other one to measure the phase of the magnetic flux density very close to the metamaterial layer, the phase and magnitude behaviors were observed using an oscilloscope.

Figure 10 shows the phase change of the magnetic flux density at 43.5 cm from the source with changing frequency. The vertical axis shows the normalized induced voltages in the coils used for monitoring. All reference signals (V_{ref}) were normalized to 2 V peak-peak and the

magnetic field signals were scaled in the same ratio to be able to compare the magnitude of magnetic field signal (V_{LPE}) at the point which is monitored, additional to the phase of the signal. Thus, both magnitudes and phases of V_{LPE} in Figure 10 are the direct measure of the real magnetic flux density signal magnitude and phase to observe the frequency response. The figures show the signal for several frequencies from 5100 Hz to 7000 Hz. It can be seen that the phase difference between the source magnetic flux density and the total magnetic flux density where the monitoring coil was placed comes from low values, passes through 180 degrees and goes towards 360 degrees with increasing frequency. Because of mutual coupling between the coils, the optimum operating frequency of the metamaterial is different from those of individual meta-atoms [29].

The frequency characteristic at 63 cm from the source coil can be seen in Figure 11. The suppressing effect of the Lattice Phase Equalizer on the below-resonance enhancement is seen clearly. Thus, the new meta-atom shows much better shielding performance (see Figure 8) and it suppresses the field enhancement below resonance. Theoretically, if a meta-atom without the phase lattice filter circuit shields the external magnetic field 80%, it enhances the external magnetic field 400% in the enhancement regime below resonance (see Equations (4) and (5)). If shielding becomes 90%, the enhancement becomes 900%. With the phase lattice filter circuit, this huge enhancement is almost entirely eliminated in the vicinity of the shielding frequency band. The

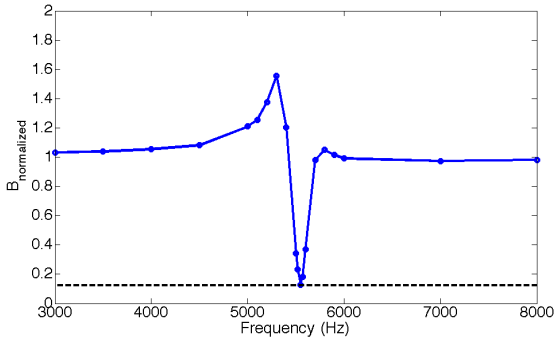

Figure 11. Frequency response of a metamaterial built by meta-atoms with two coils and lattice phase equalizer. $B_{\text{normalized}}$ is the magnetic flux density normalized to the source magnetic flux density. The suppression effect of the lattice phase equalizer on the enhancement below resonance is seen clearly.

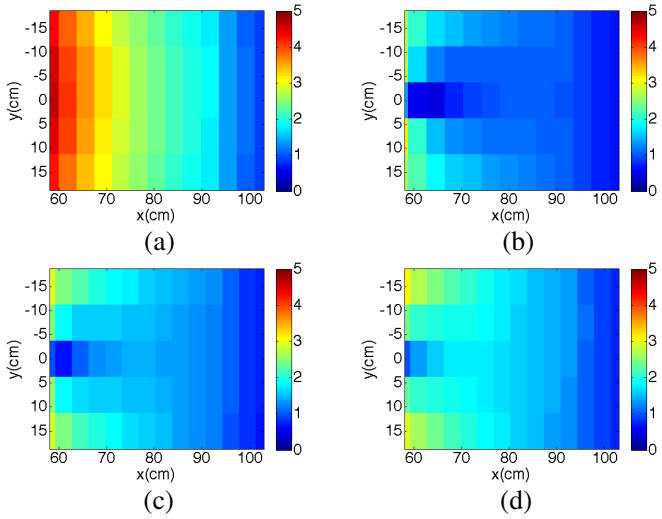

Figure 12. The spatial distribution of magnetic flux density without and with metamaterial. The color shows the magnetic flux density in μT. The source coil is at $(x = 0, y = 0)$. (a) The magnetic flux density of the source coil. (b) The magnetic flux density with the metamaterial first layer at $x = 38\,\text{cm}$ and the layer of secondary coils at $x = 14\,\text{cm}$. (c) The magnetic flux density with the metamaterial first layer at $x = 38\,\text{cm}$ and the layer of secondary coils at $x = 16.5\,\text{cm}$. (d) The magnetic flux density with the metamaterial first layer at $x = 38\,\text{cm}$ and the layer of secondary coils at $x = 19\,\text{cm}$. It is seen that the new meta-atoms improve shielding considerably (see Figure 8). It is also observed that the location of the dip point can be controlled by the position of the secondary coils.

bandwidth in which the shielding stays more than 70% of its maximum is 109 Hz. It is 55 Hz in lower frequency side and 54 Hz towards higher frequencies, which means that the shielding vs. frequency curve around the optimum shielding point is more symmetric than for the standard RLC metamaterial.

After finding the frequency (5550 Hz) at which the phase difference is 180 degree, the spatial shielding behavior of the new metamaterial is observed experimentally. The improvement in the shielding can be seen clearly in Figure 12 compared to the standard RLC metamaterial layer (Figure 8).

In the region to be shielded, there is a minimum field point, at which the metamaterial field cancels the source field. Although zero

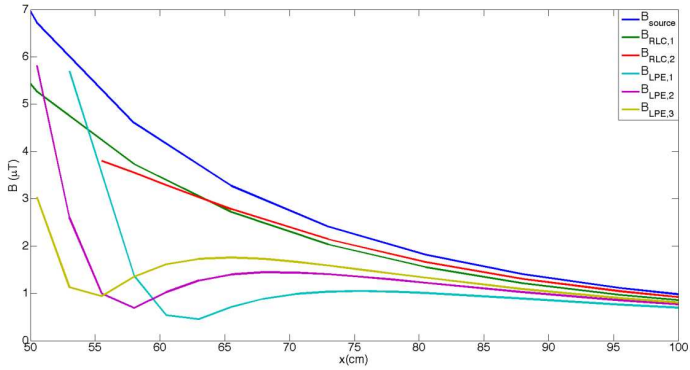

Figure 13. Magnetic flux density on the line $y = 0$. B_{source}: Magnetic flux density (B) of the source, $B_{RLC,1}$: B with metamaterial made of RLCs located at $x = 14\,\text{cm}$, $B_{RLC,2}$: B with metamaterial made of RLCs located at $x = 38\,\text{cm}$, $B_{LPE,1}$: B with metamaterial made of coil layers at $x = 14\,\text{cm}$ and $x = 38\,\text{cm}$, and lattice phase equalizer circuits, $B_{LPE,2}$: B with metamaterial made of coil layers at $x = 16.5\,\text{cm}$ and $x = 38\,\text{cm}$, and lattice phase equalizer circuits, $B_{LPE,3}$: B with metamaterial made of coil layers at $x = 19\,\text{cm}$ and $x = 38\,\text{cm}$, and lattice phase equalizer circuits.

field is expected at this point, due to alignment errors, component tolerances, ambient noise and relatively large probe size (3 cm diameter), instead of 100% shielding 87% shielding was measured at most. The distance of the minimum field point from the source is dependent on the magnitude of the current through the meta-atoms. Increasing the current through the meta-atoms, the minimum field point can be shifted to larger distances, whereas decreasing the current would shift the point towards the source. The current through the meta-atoms can be controlled by the position of the secondary coils which are responsible for the induced voltages on the meta-atoms. When these secondary coils are further away from the source coil, meta-atoms have less voltage and current, and this carries the minimum point towards the source. The spatial distribution of magnetic flux density was measured for three different secondary coil positions. In Figure 12, it is seen that by moving the secondary coils away from the source, the minimum point can be shifted towards the source.

In Figure 13, the field for different cases are plotted on the line $y = 0$ for a comparison. The improvement in the shielding and the shift of the dip point can be seen more clearly.

6. CONCLUSION

Shielding of magnetic fields at very low frequencies by means of metamaterials was studied theoretically and experimentally. A promising method to improve the shielding based on passive LC circuits with a lattice phase equalizer has been introduced, analyzed, and measured. This design does not have the drawbacks of active circuits, i.e., the resulting metamaterial is relatively cheap and has low weight and low costs. The new meta-atom shows considerably improved shielding, nice symmetry properties with respect to the maximum shielding frequency and much less undesired field enhancement below the maximum shielding frequency.

ACKNOWLEDGMENT

We would like to thank EWZ (Power supply company of Zurich) for financial support and measurement equipment.

REFERENCES

1. Shalaev, V. M., "Optical negative-index metamaterials," *Nature Photonics*, Vol. 1, No. 1, 41–48, 2007.
2. Shelby, R. A., D. R. Smith, and S. Schultz, "Experimental verification of a negative index of refraction," *Science*, Vol. 292, No. 5514, 77–79, Apr. 2001.
3. Pendry, J. B., "Negative refraction makes a perfect lens," *Phys. Rev. Lett.*, Vol. 85, No. 18, 3966–3969, Oct. 2000.
4. Liu, Z., N. Fang, T.-J. Yen, and X. Zhang, "Rapid growth of evanescent wave by a silver superlens," *Applied Physics Letters*, Vol. 83, No. 25, 5184–5186, Dec. 2003.
5. Fang, N., Z. Liu, T.-J. Yen, and X. Zhang, "Regenerating evanescent waves from a silver superlens," *Opt. Express*, Vol. 11, No. 7, 682–687, Apr. 2003.
6. Lagarkov, A. N. and V. N. Kissel, "Near-perfect imaging in a focusing system based on a left-handed-material plate," *Phys. Rev. Lett.*, Vol. 92, No. 7, 077401, Feb. 2004.
7. Fang, N., H. Lee, C. Sun, and X. Zhang, "Sub-diffraction-limited optical imaging with a silver superlens," *Science*, Vol. 308, No. 5721, 534–537, Apr. 2005.
8. Lee, H., Y. Xiong, N. Fang, W. Srituravanich, S. Durant, M. Ambati, C. Sun, and X. Zhang, "Realization of optical

superlens imaging below the diffraction limit," *New Journal of Physics*, Vol. 7, 255–255, Dec. 2005.

9. Zhang, X. and Z. Liu, "Superlenses to overcome the diffraction limit," *Nat. Mater.*, Vol. 7, No. 6, 435–441, Jun. 2008.
10. Pendry, J. B., D. Schurig, and D. R. Smith, "Controlling electromagnetic fields," *Science*, Vol. 312, No. 5781, 1780–1782, Jun. 2006.
11. Raton, B., et al., *Power Frequency Magnetic Fields and Public Health*, CRC Press, 1995.
12. Boyvat, M. and C. V. Hafner, "Molding the flow of magnetic field with metamaterials: Magnetic field shielding," *Progress In Electromagnetics Research*, Vol. 126, 303–316, 2012.
13. Solymar, L. and E. Shamonina, *Waves in Metamaterials*, Oxford University Press, 2009.
14. Cui, T. J., D. R. Smith, and R. Liu, *Metamaterials: Theory, Design, and Applications*, Springer, 2010.
15. Xu, W., W. J. Padilla, and S. Sonkusale, "Loss compensation in Metamaterials through embedding of active transistor based negative differential resistance circuits," *Opt. Express*, Vol. 20, No. 20, 22406–22411, Sep. 2012.
16. Dong, Z.-G., H. Liu, T. Li, Z.-H. Zhu, S.-M. Wang, J.-X. Cao, S.-N. Zhu, and X. Zhang, "Optical loss compensation in a bulk left-handed metamaterial by the gain in quantum dots," *Applied Physics Letters*, Vol. 96, No. 4, 044104-044104–3, Jan. 2010.
17. Xiao, S., V. P. Drachev, A. V. Kildishev, X. Ni, U. K. Chettiar, H.-K. Yuan, and V. M. Shalaev, "Loss-free and active optical negative-index metamaterials," *Nature*, Vol. 466, No. 7307, 735–738, Aug. 2010.
18. Soukoulis, C. M. and M. Wegener, "Optical metamaterials — More bulky and less lossy," *Science*, Vol. 330, No. 6011, 1633–1634, Dec. 2010.
19. Jelinek, L. and J. Machac, "An FET-based unit cell for an active magnetic metamaterial," *IEEE Antennas and Wireless Propagation Letters*, Vol. 10, 927–930, 2011.
20. González-Posadas, V., D. Segovia-Vargas, E. Ugarte-Muñoz, J. L. Jiménez-Martín, and L. E. García-Muñoz, "On the performance of negative impedance converters (NICs) to achieve active metamaterials," *ICECom, 2010 Conference Proceedings*, 1–4, 2010.
21. Tretyakov, S. A., "Meta-materials with wideband negative permittivity and permeability" *Microwave and Optical Technology*

Letters, Vol. 31, No. 3, 163–165, 2001.

22. Zhang, S., W. Fan, K. J. Malloy, S. R. J. Brueck, N. C. Panoiu, and R. M. Osgood, "Demonstration of metal-dielectric negative-index metamaterials with improved performance at optical frequencies," *J. Opt. Soc. Am. B*, Vol. 23, No. 3, 434–438, Mar. 2006.
23. Shalaev, V. M., W. Cai, U. K. Chettiar, H.-K. Yuan, A. K. Sarychev, V. P. Drachev, and A. V. Kildishev, "Negative index of refraction in optical metamaterials," *Opt. Lett.*, Vol. 30, No. 24, 3356–3358, Dec. 2005.
24. Tretyakov, S., *Analytical Modeling in Applied Electromagnetics*, Artech House, 2003.
25. Sussman-Fort, S. E. and R. M. Rudish, "Non-Foster impedance matching of electrically-small antennas," *IEEE Transactions on Antennas and Propagation*, Vol. 57, No. 8, 2230–2241, Aug. 2009.
26. Boillat, D. O., T. Friedli, and J. W. Kolar, "Electronically controllable impedance for tuning of active metamaterials," *IECON 2011 — 37th Annual Conference on IEEE Industrial Electronics Society*, 1335–1341, 2011.
27. Johnson, D. E., *Introduction to Filter Theory*, Prentice-Hall, 1976.
28. Bakshi, U. A., *Telecommunication Engineering*, Technical Publications, 2009.
29. Shamonina, E. and L. Solymar, "Diamagnetic properties of metamaterials: A magnetostatic analogy," *Eur. Phys. J. B*, Vol. 41, No. 3, 307–312, Oct. 2004.